Solid State Communications 149 (2009) 1292–1295

Contents lists available at ScienceDirect

Solid State Communications

journal homepage: www.elsevier.com/locate/ssc

Growth and magnetic properties of the sandwich structure Fe/magnetic silicide/Si(100) obtained from in situ optic and magneto-optic data

A.S. Gouralnik [a,*], N.G. Galkin [a], D.L. Goroshko [a], S.A. Dotsenko [a], A.A. Alekseev [a], V.A. Ivanov [b]

[a] Institute for Automation and Control Processes FEB RAS. 5, Radio. Street 690041, Vladivostok, Russia

[b] Far East State University. 8, Sukhanova Street, 690000, Vladivostok, Russia

ARTICLE INFO

Article history:
Received 19 February 2009
Received in revised form
9 April 2009
Accepted 7 May 2009 by C. Lacroix
Available online 14 May 2009

PACS:
75.75.+a
78.66.Bz
78.20.Jq
78.40.-q

Keywords:
A. Iron
A. Magnetic silicide
A. Silicon
E. Kerr effect

ABSTRACT

It is demonstrated by the Surface Magneto-Optic Kerr Effect and Differential Reflectance Spectroscopy methods that structures free of magnetically dead layers can be created by the deposition of iron at room temperature onto a prefabricated magnetic silicide layer. The magnetic silicide can be formed by the deposition of iron at 70 °C onto a layer of amorphous silicon prefabricated on Si(100). Both in the silicide and the iron film, magnetism onsets after the iron amount deposited reaches some critical value. The spontaneous magnetization vector in the iron film changes its direction twice during the film growth. Sufficiently thick iron films persist being ferromagnetic in air for years.

1. Introduction

In recent years much attention has been paid to the investigation of the growth processes and properties of thin iron films on silicon surfaces. The complexity of this system, which is multicomponent at the very early stages of growth due to material intermixing and structural transformations, represents a great scientific challenge [1–10]. From the technological point of view, iron films look promising as possible magnetic memory media integrated in the traditional silicon technology. Possible applications of such films in spintronics are of great interest [9,10].

Despite much information that has been accumulated and significant progress that has been achieved in studies of the growth mechanism, full understanding of the process of iron growth on silicon is far from completion. The results obtained in experiments are sometimes different. This is explained by a few reasons of which two seem particularly significant. First, the substrates used in experiments differ in their crystalline quality, doping impurity type and concentration, etc. Second, the surface preparation methods used also differ, resulting in different properties of the heterogeneous real surfaces. The physical and chemical processes taking place on these surfaces during iron deposition can differ significantly, resulting in different properties of the deposited films, including their ferromagnetism.

One of the major problems is intermixing of iron deposited onto the surface with the silicon substrate. The heterogeneous interface formed in this process represents a magnetically dead layer, hampering the injection of spin-polarized electrons into the silicon for further processing.

It has been demonstrated in [4,5] that prefabricated templates of β-$FeSi_2$ or $CoSi_2$ efficiently block the interdiffusion and promote the epitaxial growth of the iron film. Nevertheless, these silicides represent magnetically dead layers.

In the present work an attempt is made to create a similar structure free of a magnetically dead layer. It is suggested to separate the ferromagnetic iron film from the substrate by a thin *magnetic* layer produced by the deposition of amorphous silicon (a-Si) which is subsequently transformed into magnetic silicide by iron deposition onto the slightly heated substrate. Thus, we study two items: the transformation of a-Si into the magnetic silicide and the growth of iron upon this silicide.

* Corresponding author. Tel.: +7 4232 320682; fax: +7 4232 310452.
E-mail address: fun_era@mail.ru (A.S. Gouralnik).

0038-1098/$ – see front matter © 2009 Elsevier Ltd. All rights reserved.
doi:10.1016/j.ssc.2009.05.009

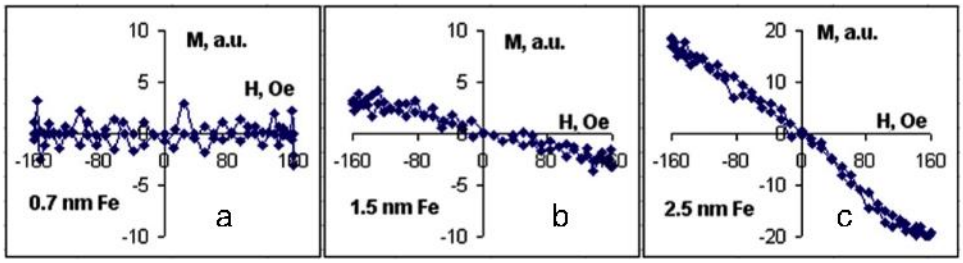

Fig. 1. SMOKE loops registered from an Fe film growing at $T \sim 70$ °C on a 1.4 nm thick (~10 ML) a-Si layer prefabricated on a Si(100) substrate.

2. Experimental

The experiments were carried out in a UHV chamber with the base vacuum of $2–4 \times 10^{-10}$ Torr, equipped with original units for investigating the Surface Magneto-Optic Kerr Effect (SMOKE) [11] and Differential Reflectance Spectroscopy (DRS) [12]. Fe and Si evaporation sources, a manipulator with a sample holder for three samples and a quartz microbalance.

Silicon samples were cleaned in UHV conditions by DC heating at 600 °C for 4–5 h and then by flashing a few times at 1250 °C.

Iron was deposited either at discrete doses, at the rate 0.7 nm/min (SMOKE experiments), or continuously, at the rate 0.012 nm/min (DRS experiments) from AC-heated tungsten spirals. Amorphous silicon was deposited at the rate 3.5 nm/min from a silicon sublimation source. Both evaporators were preliminarily well outgassed. The deposition rates were pre-calibrated with a quartz microbalance. For convenience, hereafter the deposit amount is expressed in nanometers and monolayers (1 ML $= 6.8 \times 10^{14}$ cm^{-2}).

For the silicide growth, during iron deposition onto the prefabricated a-Si layer the substrate was slightly heated by a DC current. Estimation of the temperature was made based on the Fick equation and Stephan–Boltzman law accounting for energy dissipation due to the heat sink and irradiation from the sample, respectively. According to our estimation, the temperature of the substrate attached to the massive stainless steel sample holder by Ta clips increased within the range ~(55–70) °C during each deposition cycle, the estimation error being of about 40 °C. The highest estimation value of 70 °C is used in the text below.

To study the ferromagnetism of the film, an original SMOKE installation [11] was used. It has a vacuum-tight system of two pairs of electromagnets allowing in situ measurements of both the longitudinal and transversal magneto-optic Kerr effects. In the present work the longitudinal effect was measured with the field applied along $[100]_{Si}$.

To study the optical functions of the growing film, the original DRS unit was used. This method is based on permanent monitoring of optical reflectance from the surface during the film growth [12].

3. Results and discussions

3.1. SMOKE study of the magnetic silicide layer growth on an a-Si layer at 70 °C

First, a 1.4 nm thick (~10 ML) silicon layer was deposited at the rate of 3.5 nm/min onto a clean Si(100) surface at room temperature (RT); according to [13], the silicon deposited under these conditions was amorphous (a-Si). Then four doses of iron (0.7 nm, 0.8 nm, 0.5 nm and 0.5 nm) were deposited at $T \sim 70$ °C upon the a-Si layer, with SMOKE measurements after each deposition.

The SMOKE results are given in Fig. 1. It is seen from the first SMOKE loop (Fig. 1(a)) that after deposition of 0.7 nm (~8.5 ML) of Fe onto the 1.4 nm thick (~10 ML) a-Si layer at the moderate temperature of ~70 °C the film remained non-magnetic. After adding another 0.8 nm of Fe, some feature of magnetic susceptibility occurred (Fig. 1(b)) that became more prominent after deposition of the next Fe doses (see Fig. 1(c), showing the loop obtained after the fourth deposition).

It is interesting to compare our data to the results by Berling et al. [6] for a film obtained by co-deposition of Fe and Si, where spontaneous magnetization (SM) was observed in the mixture with the average composition $Fe_{1.35}Si$. Suggesting that the $Fe_{1.35}Si$ stoichiometry is sufficient for the occurrence of magnetism, we estimate that in our experiment the iron distribution in a-Si after the first deposition of 0.7 nm must extend deeper than 0.9 nm (6–7 ML); otherwise, SM should be observed. The silicide formed in this Fe-deficit mixture was non-magnetic FeSi, as shown below (Section 3.3).

Observation of magnetism for iron thickness $d_{Fe} \sim 1.5$ nm (average stoichiometry $Fe_{1.8}Si$)) indicates the occurrence of some ferromagnetic phase (Fig. 1(b); we suggest, it is Fe_3Si, since our DRS data (see Section 3.3) show the absence of iron and the presence of Fe_3Si for this average stoichiometry. This is in agreement with the XPS data [7] and magnetic linear dichroism combined with XPS data [8], where spectroscopic features of Fe_3Si were marked and ferromagnetism observed upon 0.7 nm iron deposition at RT on Si(100) 2×1 and annealing at temperatures below 100 °C.

After the next depositions, for the film with the effective stoichiometry close to Fe_3Si, the magnetism is more prominent (Fig. 1(c)), indicating that the volume of the Fe_3Si phase is larger. Nevertheless, the shape of the loop is characteristic of a superparamagnetic material rather than a ferromagnetic one.

It is known from STM data [3] that iron films of thickness $0 < d_{Fe} < 15$ ML obtained by the SPE method at moderate annealing temperatures (below 200 °C) consist of ~1 nm size islands. We suppose that the magnetic phase Fe_3Si formed in our experiment at $T \sim 70$ °C and $d_{Fe} \sim (1.5–2.5)$ ML also had the shape of very small granules that are superparamagnetic at RT. Upon increasing the deposited Fe amount, the particles grew in size, resulting in an increase of magnetic susceptibility. Possibly, the material gradually became enriched with iron (the Fe content in the Fe_3Si lattice can reach 91%). Nevertheless, being very small, the granules remained superparamagnetic.

3.2. Growth of the iron film on the magnetic silicide surface at RT

To study the process of formation of a ferromagnetic iron film on the prefabricated silicide described in the previous section, a few doses of iron were deposited at RT onto the silicide surface with SMOKE measurements after each deposition. The evolution of SMOKE loops for $0.5 < d_{Fe} < 5.2$ nm is shown in Fig. 2.

In agreement with [14], we attribute the V-shaped loop (Fig. 2(a)) to the superposition of polar and longitudinal Kerr effects. In fact, SM with the easy magnetization axis perpendicular to the surface is usually the first to onset in the growing iron films [1,4,5]. In our setup, this SM could cause some polar Kerr effect mixed with the longitudinal effect due to the presence of some perpendicular component in the longitudinal magnetic field.

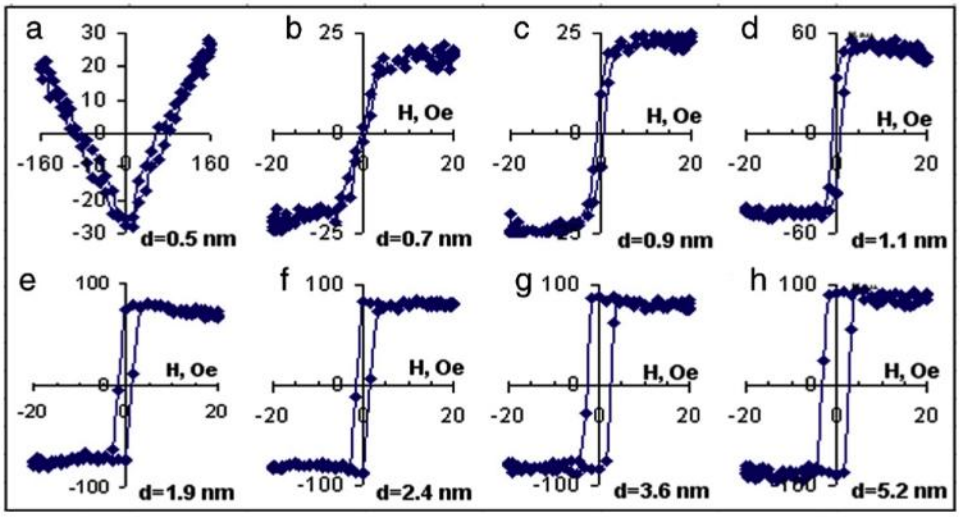

Fig. 2. SMOKE loops for different stages of iron film growth on the silicide surface at RT.

The shape of the SMOKE loop in Fig. 2(b) is characteristic for the *hard* magnetization axis oriented along the $[100]_{Si}$ direction. Evolution of the loop shape during further deposition shows rotation of the magnetization vector for the range 0.7 nm $< d_{Fe} <$ 1.1 nm, so that the direction $[100]_{Si}$ finally becomes the *easy* magnetization axis. After completion of depositions, transversal SMOKE loops with magnetic field applied along $[010]_{Si}$ were recorded. These loops (not shown here) had the same shape as the rectangular longitudinal loops given in Fig. 2(g) and (h). Hence, both $[100]_{Si}$ and $[010]_{Si}$ are *easy* magnetization directions, at least for films thicker than 1.9 nm.

Thus, the sequence of magnetization vector rotations is similar to that reported in [1,6]: (1) occurrence of SM normal to the surface, (2) rotation of the SM vector to the in-plane direction with the *hard* axis along $[100]_{Si}$, (3) in-plane rotation of the *easy* magnetization vector to the $[100]_{Si}$ direction. It should be mentioned that the in-plane rotation was observed in [6] at higher iron thickness (2.5–2.9 nm) for an iron film growing upon an epitaxial β-$FeSi_2$ layer prefabricated on the Si(100) surface. The authors explained this rotation by the magneto-elastic effect due to relaxation of the elastic stress in the interface. In our experiment, similar rotation was observed at an earlier stage of deposition. This can be explained by the disordered granular structure of the prefabricated silicide layer. Another phenomenon that is also involved in the magnetization rotation process could be the occurrence of exchange interactions between neighboring islands when their size becomes large enough and the separation distance shortens.

Further increase of the iron thickness results in an increase of the coercive force H_c from 0.5 Oe up to 3 Oe (see Fig. 3(b)–(h)) and loop rectangularity M_r/M_s from 0.07 up to 1 (see Fig. 3(b)–(e)).

A simple but practically important observation is noteworthy: our ex situ MOKE data evidence that the ferromagnetic properties of this sample have persisted for 5 years since it was unloaded from the UHV chamber. In contrast, multiple Fe/Si films thinner than 2 nm lost their magnetic properties in the air very quickly. This is naturally explained by the fast oxidation of the film material. Thus, we can conclude that the oxidized layer extends to a depth of about 2 nm and represents a diffusion barrier hampering further oxidation. This simple observation can be important in applications.

3.3. DRS study of the iron silicide formation on an a-Si layer at 70 °C

The reflectance spectra in the range of 1.13–2.51 eV were recorded every 10 s during iron deposition on the prefabricated a-Si layer at 70 °C. The DRS method gives the imaginary part of the dielectric function ε'' from the $\Delta R/R$ curves for the regions where the dependence $\Delta R/R$ versus d_{Fe} is linear [12]. To separate these regions in the best way, digital differentiation of curves for all photon energies was used because our DRS data processing method is sensitive to the linearity of the dependence and the number of experimental points within the chosen region. To be sure that no new phases (i.e. no linear regions with different slope) occur, the d_{Fe} range was extended to 3 nm, besides 2.5 nm as in experiments on magnetism. The curves of $\Delta R/R$ versus d_{Fe} for three photon energies are given in Fig. 3(a) as examples. Two linear regions were separated on the plots and the imaginary part of the dielectric function $\varepsilon''(E)$ was calculated for these regions (Fig. 3(b)).

For interpretation of the DRS curves, first-principles Density Functional Theory computer modeling of the Fe/Si system was carried out with the FHI96SPIN software [15]. Based on the positions of peaks in the calculated distributions of density of states, one could expect optical transition energies of 1.2, 1.9 and 2.2 eV for ε-FeSi and 1.5, 2 and 2.5 eV for Fe_3Si.

The positions of the broad peaks in curves 1 and 2 (Fig. 3(b)) agree satisfactorily with those expected for the transition energies calculated for ε-FeSi and some mixture of Fe_3Si with ε-FeSi, respectively. We attribute the downward shift of the whole curve 2 to the occurrence of Fe_3Si in the film. The ε'' increase at higher energies can be attributed to transitions in silicon. Taking into account the above SMOKE data, the positions of the peaks and the positions of the whole curves, we conclude that for $d_{Fe} < 1.4$ nm the compound consists mostly of ε-FeSi (Fig. 3(b), curve 1) and for $d_{Fe} > 1.4$ nm (Fig. 3(b) curve 2) it contains small granules of Fe_3Si whose total volume gradually increases with d_{Fe}. We suppose that the interface a-Si/substrate remains sharp because iron intermixing with a-Si is much faster than with the substrate and deeper layers are less abundant in iron atoms, especially after the formation of dense silicides upon them.

3.4. DRS study of RT iron growth on the magnetic silicide layer

Iron was deposited at RT onto the surface of the silicide grown in the previous stage and the $\Delta R/R$ versus d_{Fe} dependence recorded. Three regions, (1), (2) and (3), were separated on the plots of $\Delta R/R$ versus d_{Fe}. The intermediate region (2) is not considered here since it does not meet the linearity criterion. The curves of $\Delta R/R$ versus d_{Fe} and ε'' versus photon energy are presented in Fig. 4(a) and (b), respectively. In addition, the curve for pure iron calculated from the data in [16] is given in Fig. 4(b).

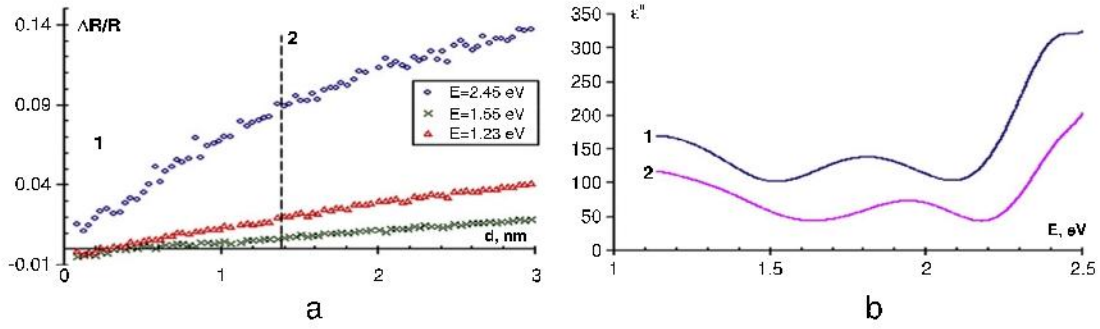

Fig. 3. (a) $\Delta R/R$ curves measured during iron deposition onto a-Si at 70 °C. (b) Imaginary part of the dielectric function versus photon energy.

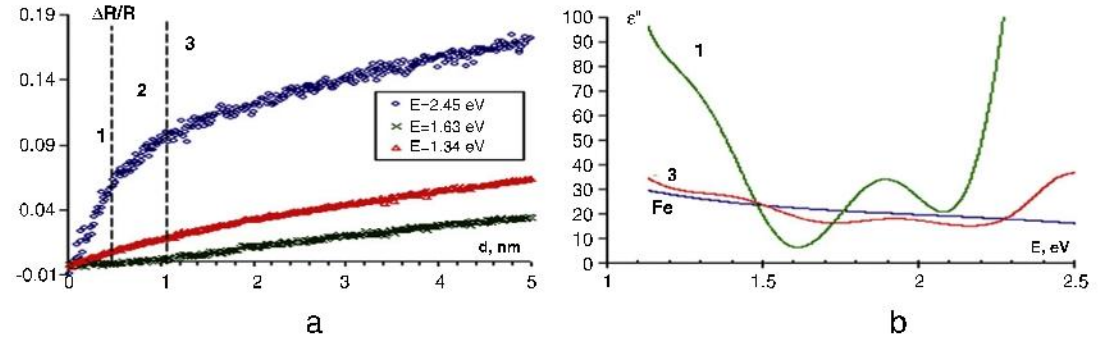

Fig. 4. (a) The curves of $\Delta R/R$ measured during RT iron deposition onto the prefabricated magnetic silicide. (b) Imaginary part of the dielectric function versus photon energy.

The shape of the curve 1 (peaks and curve position) indicates that for $d_{Fe} < 1.1$ nm the growing substance is mainly Fe_3Si. This is natural, since the average stoichiometry of the compound is close to Fe_4Si and, as we mentioned above, the homogeneity range of the Fe_3Si lattice is very wide. Since the reflected light escape depth is large (~20 nm) and the features of ε-FeSi in curve 1 are very weak, as compared to the curves in Fig. 3(b), we can conclude that at this stage of deposition the Fe_3Si thickness increases (at least partly) at the expense of the ε-FeSi layer formed before. Transformation of ε-FeSi into Fe_3Si in the Fe-rich environment is possible because the Fe_3Si formation enthalpy is larger than that for ε-FeSi (93.8 kJ/mol and 81.2 kJ/mol, respectively). We suppose that at this stage of deposition iron still penetrates into the silicide layer, with transformation of ε-FeSi into Fe_3Si, but it does not penetrate deeper, otherwise features of newly formed FeSi (high-level position of the curve and peak energies) would be seen. Thus, we suppose that the silicide layer formed at earlier stages of deposition is thick and dense enough to block the penetration of iron into the silicon substrate.

It is seen in Fig. 4(b) that both the position and slope of curve 3 are very similar to those for the curve for pure iron. Nevertheless, peaks related to Fe_3Si are also seen. This observation allows us to conclude that for $d_{Fe} > 1.1$ nm (average stoichiometry $Fe_{4.8}Si$) the deposited film consists mainly of iron and Fe_3Si. Weakening of the Fe_3Si features is attributed to the transformation of some part of the silicide into iron.

4. Conclusions

1. Magnetic silicide Fe_3Si can be formed on the surface Si(100) by the deposition of iron onto a pre-deposited a-Si layer at slightly increased temperature. This material is superparamagnetic at RT, probably because it consists of small granules.

2. A ferromagnetic film can be grown on the surface of the above silicide. The evolution of its ferromagnetic asymmetry has the following stages: (1) occurrence of spontaneous magnetization normal to the surface, (2) rotation of the spontaneous magnetization vector to the in-plane direction with the *hard* axis along $[100]_{Si}$, (3) in-plane rotation of the *easy* magnetization vector to the $[100]_{Si}$ direction.

3. Iron films deposited onto silicon or silicide surface persist being ferromagnetic for years if they are thick enough ($d_{Fe} \sim$ 3.5–5 nm).

Acknowledgements

This work was supported by Russian Fund for Basic Researches (Grants 09-02-98501-P_BOCTOK and 07-02-00958_a).

References

[1] Z.H. Nazir, C-K. Lo, M. Hardiman, JMMM 156 (1996) 435–436.
[2] J. Chrost, J.J. Hinarejos, P. Segovia, E.G. Michel, R. Miranda, Surf. Sci. 371 (1997) 287–306.
[3] H. Nakano, K. Maetani, K. Hattori, H. Daimon, Surf. Sci. 601 (2007) 5088–5092.
[4] P. Bertoncini, P. Wetzel, D. Berling, A. Mehdaoui, B. Loegel, G. Gewinner, R. Poinsot, V. Pierron-Bohnes, JMMM 237 (2001) 191–205.
[5] P. Bertoncini, P. Wetzel, D. Berling, G. Gewinner, C. Ulhaq-Bouillet, V. Pierron-Bohnes, Phys. Rev. B 60 (1999) 11123–11130.
[6] D. Berling, G. Gewinner, M.C. Hanf, K. Hricovini, S. Hong, B. Loegel, A. Mehdaoui, C. Pirri, M.H. Tuilier, P. Wetzel, JMMM 191 (1999) 331–3386.
[7] R. Klasges, C. Carbone, W. Eberhardt, C. Pampuch, O. Rader, T. Kachel, W. Gudat, Phys. Rev. B 56 (17) 10801–10804.
[8] I.I. Pronin, M.V. Gomoyunova, D.E. Malygin, D.V. Vyalikh, Yu.S. Dedkov, S.L. Molodtsov, J. Appl. Phys. 104 (2008) 104914.
[9] J.V. Barth, G. Costantini, K. Kern, Nature 437 (2005) 673.
[10] F. Zavaliche, M. Przybylski, W. Wulfhekel, J. Grabovski, R. Scholz, J. Kirschner, Surf. Sci. 507–510 (2002) 560–566.
[11] A.S. Guralnik, N.G. Galkin, D.L. Goroshko, V.A. Ivanov, A.M. Maslov, I.V. Soppa, T.V. Turchin, W. Park, Y. Park, Instr. & Experimental Techniques 49 (6) (2006) 834–838.
[12] S.A. Dotsenko, N.G. Galkin, A.S. Gouralnik, I.V. Koval', e-J. Surf. Sci. Nanotech. 3 (2005) 113.
[13] H. Jorke, H.-J. Herzog, H. Kibbel, Phys. Rev. B 40 (1989) 2005.
[14] H.F. Ding, S. Putter, H.P. Oepen, J. Kirschner, Phys. Rev B 63 134425.
[15] R. Car, M. Parrinello, Phys. Rev. Lett. 55 (1985) 2471.
[16] J.H. Weaver, E. Colavita, D.W. Lynch, R. Rosei, Phys. Rev. B 19 (8) 3850–3856.